ELSEVIER

Journal of Nuclear Materials 302 (2002) 156–164

journal of nuclear materials

www.elsevier.com/locate/jnucmat

Application of neutron radiography for estimating concentration and distribution of hydrogen in Zircaloy cladding tubes

Ryou Yasuda [a,*], Masahito Matsubayashi [b], Masahito Nakata [a], Katsuya Harada [a]

[a] *Department of Hot Laboratories, Japan Atomic Energy Research Institute, Tokai-mura, Naka-gun, 319-1195 Ibaraki-ken, Japan*
[b] *Center for Neutron Science, Japan Atomic Energy Research Institute, Tokai-mura, Naka-gun, Ibaraki-ken 319-1195, Japan*

Received 16 January 2001; accepted 19 January 2002

Abstract

Practicability of neutron imaging plate (IP) and computed tomography (CT) for estimating the distribution of the hydrogen concentration in Zircaloy tubes was investigated. Zircaloy tubes with controlled amount of hydrogen which is segregated at the periphery were prepared. The width of the hydrogen region is small around 0.1 mm. In IP image the small segregated hydrogen region is recognized, and the distribution of the hydrogen in the Zircaloy tubes is displayed. The hydrogen region is also recognized in a CT image of the tube containing large amount of hydrogen. These results show that both neutron IP and CT methods are applicable tools to estimate hydrogen distribution. A quantitative evaluation of the hydrogen concentration by those images is also discussed.

PACS: 28.52.Fa; 29.30.Hs; 28.50.Dr

1. Introduction

Hydrogen embrittlement of a Zircaloy cladding tube is one of the important issues from the viewpoint of fuel safety. It is well known that hydrogen embrittlement is caused by a high concentration of hydrogen. The hydrogen is introduced into Zircaloy tube under a corrosive environment with high temperature and pressurized water. Information about hydrogen behavior in a Zircaloy tube is required to improve resistance to hydrogen embrittlement in the tube. High temperature extraction method and metallographic observation of an acid-etched sample have been used to estimate the distribution of hydrogen concentration in post irradiation examination (PIE). However, these methods have limited the size of samples, and are accompanied by irreversible and complicated processes.

Neutron radiography (NRG) has been used as an effective tool for estimating hydrogen distribution in an object [1–3]. The distribution of hydrogen concentration in Zircaloy tubes has been qualitatively investigated by using an X-ray film with a metal converter in a previous work [4]. The conventional methods in NRG need long exposure time because of the low sensitivity of the films. Moreover it is difficult to estimate hydrogen concentration from the image because of its narrow dynamic range. New techniques of NRG such as neutron imaging plate (IP) and neutron TV methods have been developed in recent years [5,6]. The high sensitivity and wide dynamic range of the IP make it possible to shorten the exposure time, to perform quantitative evaluation, and to display images without complicated film development processes. The neutron TV method is feasible for an application to computed tomography (CT) method requiring a number of images to make a CT image. The

* Corresponding author. Tel.: +81-29 282 5727; fax: +81-29 282 5293.
E-mail address: yasuda@dhl.tokai.jaeri.go.jp (R. Yasuda).

0022-3115/02/$ - see front matter
PII: S0022-3115(02)00778-X

CT method is effective to obtain information about the cross-section of an object without destructive treatments.

In the present work Zircaloy cladding tubes with introduced hydrogen were prepared and examined using the neutron IP and CT methods, and the practicality of these techniques for estimating hydrogen concentration and distribution is investigated and discussed.

2. Experimental

Zircaloy-4 tubes are used in this work. The nominal composition of Zircaloy-4 is given in Table 1. The hydrogen uptake treatment was preformed at around 700 K in an atmosphere of mixture gases of hydrogen and argon. The treated tube is called hydrided tube in the following. Three hydrided tubes with different hydrogen concentrations were prepared and named as ZryH-1, ZryH-2 and ZryH-3. The concentrations are ZryH-1< ZryH-2 < ZryH-3. As shown in Fig. 1 hydrogen in the tubes was segregated in the outer-circumference region at around 0.1 mm in thickness to imitate the irradiated claddding tube. The hydrogen concentrations averaged over the thickness of the tubes were obtained by using the high temperature extraction method. The samples for hydrogen measurement were cut from both edges of the tubes and divided into two equal parts as shown in Fig. 2. The measured hydrogen concentrations of each part in the tubes are given in Table 2. There is a gradient of the measured hydrogen concentration along the length of the tube. The hydrogen concentration at the segregated area in the hydrided tubes is investigated by Nagase et al. [7]. According to the work of Nagase, the concentrations at the segregated area are around twice or three times larger than the measured average hydrogen concentration over the thickness.

NRG tests were performed at the second thermal neutron radiography facility (TNRF-2) in JRR-3M. TNRF-2 is used for only nonradioactive samples, and is equipped with a high flux neutron beam of 1.2×10^8 n/cm^2/s and a high collimator ratio of 153.

Two kinds of IP tests were performed on the hydrided tubes along with a reference tube which is not hydrided. One underwent radiography of rod images, and the other radiography of ring images. The exposure time was 4 s. The hydrided tubes for the test of the ring image were 5 mm in thickness and cut from the inlet side of the tubes. An IP of IP: BAS-ND-2025 (made by

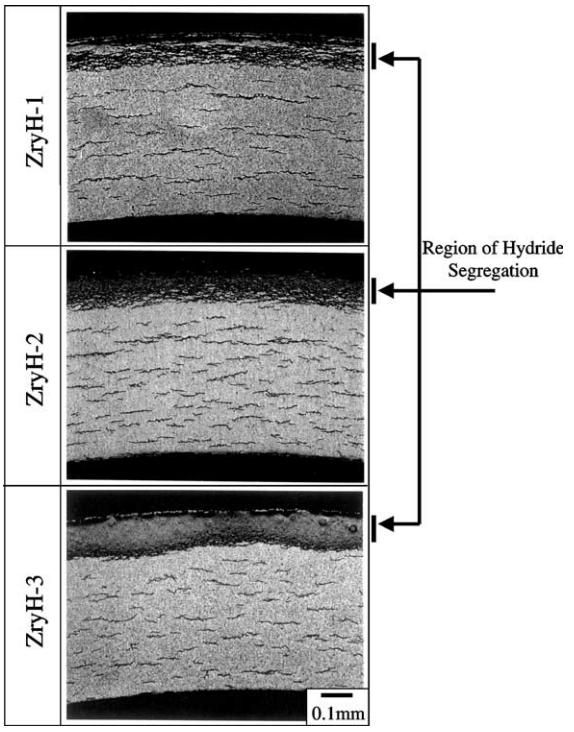

Fig. 1. Optical micrographs showing hydride segregation at outer–circumference in cross-section of Zircaloy cladding tubes. Samples were etched to show the location of hydride. Sample ID refer to Table 2.

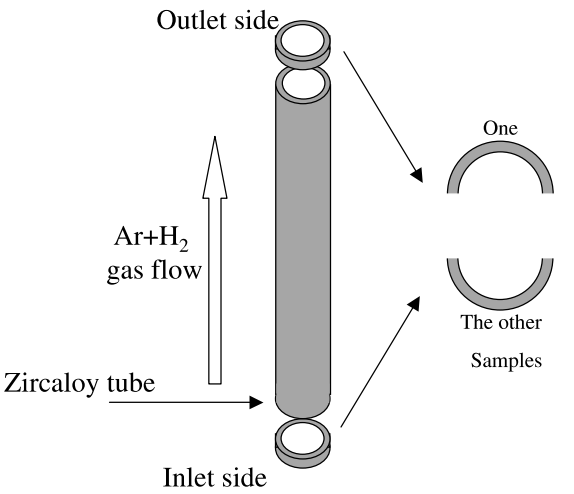

Fig. 2. Schematic drawing of sample preparation for hydrogen analysis.

Table 1
Nominal composition of Zircaloy-4 (wt%)

Composition	Zr	Sn	Fe	Cr	Ni	O	H
Zircaloy-4	Bulk	1.20–1.70	0.18–0.24	0.07–0.13	<0.007	–	<0.0025

Table 2
Hydrogen concentrations of the hydrided tubes

ID	Samples	Measured values (wt ppm)	
		Inlet side	Outlet side
ZryH-1	One	379	238
	The other	526	232
	Average	453	235
ZryH-2	One	597	483
	The other	892	513
	Average	744	498
ZryH-3	One	2032	1436
	The other	2011	786
	Average	2021	1110
Ref.	Average	17	

Fuji film) was used. The hydrided tubes were directly fixed to the surface of an IP cassette with aluminum tapes for increasing sharpness in the image. The test arrangements of IP methods are shown in Fig. 3(a) and (b). IP reader called BAS-2000 with the spatial resolution of 0.1 mm × 0.1 mm was used.

CT method was performed by a neutron TV system equipped with a cooling type CCD camera and with a ^{6}LiF:ZnS(Ag) converter. Fig. 3(c) shows the arrangement of a CT method. The 180 pieces of the rod image were continuously obtained by taking a rod image after rotating the tube in every 1° from 0° to 179° in order to reconstruct CT images. In taking a rod image, the exposure time was 7.5 s. Thickness of one layer of the CT image corresponds to 0.04 mm as shown in Fig. 3(c), and the spatial resolution of the CT image is

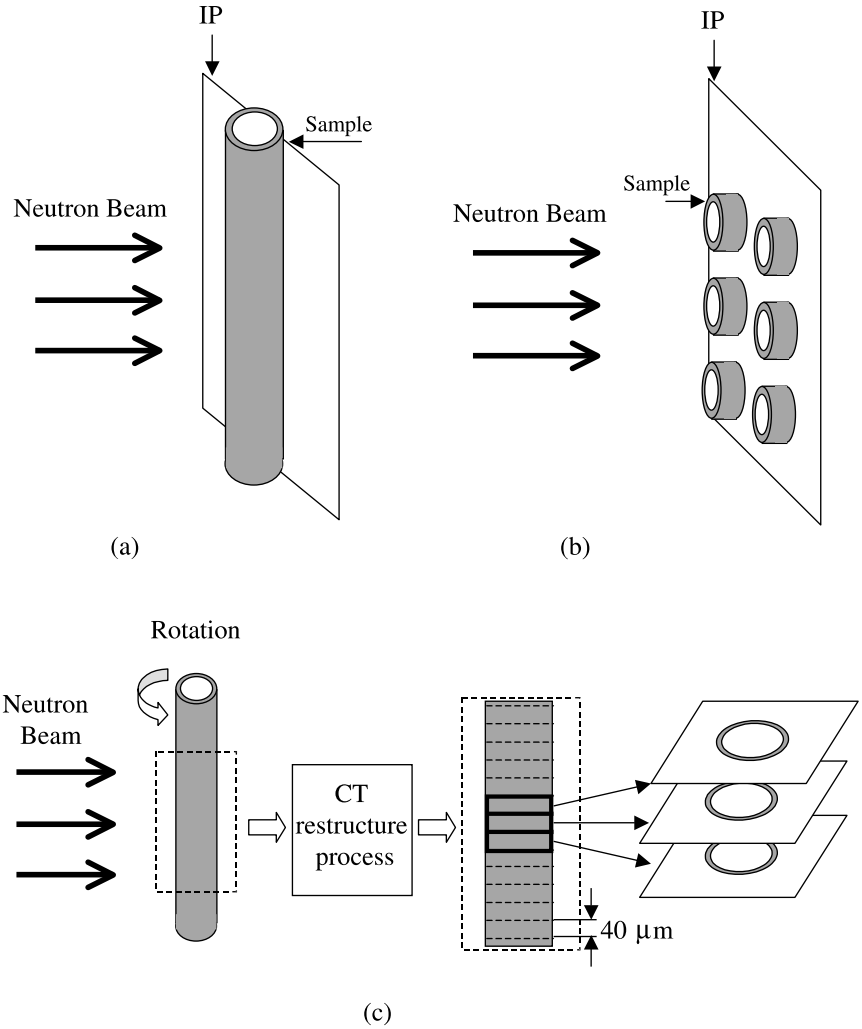

Fig. 3. Arrangements of examination of IP and CT methods. (a) and (b) show arrangement of IP method for the rod images and the ring images, respectively. (c) shows arrangement of CT method.

0.04 mm × 0.04 mm. Details of the neutron CT method are stated in the literature [8].

Software called IP-lab on a personal computer was used for image analyses. The images of IP and CT are represented as numerical data determining the contrast in the images. The numerical data of IP image is called photo-simulated luminescence (PSL) proportional to fluence of the neutron beam reached at the IP surface. The numerical data of CT image are called CT number corresponding to the attenuation coefficient of an object.

The flux of neutron beam transmitting the objects is expressed in the following Eq. (1):

$$I_s = I_0 \exp(-\Sigma t), \tag{1}$$

where I_s is the transmitted neutron flux, I_0 the initial neutron flux, Σ the macroscopic cross-section of sample, and t the length of transmittance. Eq. (1) becomes as follows:

$$\frac{I_s}{I_0} = \exp(-\Sigma t). \tag{2}$$

I_s/I_0 is given by the ratio of the PSL of the sample image to that of no sample image. Hence, Eq. (2) can be re-written as

$$\frac{\mathrm{PSL}_{\mathrm{image}}}{\mathrm{PSL}_{\mathrm{back}}} = \exp(-\Sigma t). \tag{3}$$

Eq. (3) shows that ratio of the PSLs depends on the macroscopic cross-section in the samples. The macroscopic cross-section is expressed in the following equation:

$$\Sigma = \sum_i \sigma_i N_i, \tag{4}$$

where σ_i and N_i are microscopic cross-section and density of the ith element in the object, respectively. Evaluations of the hydrogen concentrations in the hydrided Zircaloy tubes is based on the Eqs. (3) and (4).

3. Results and discussion

3.1. Imaging plate

Fig. 4 shows a rod image of the hydrided tubes and line profiles of $\mathrm{PSL}_{\mathrm{image}}/\mathrm{PSL}_{\mathrm{back}}$ in three positions. No appreciable difference in the contrast is confirmed among the images of the reference, ZryH-1 and ZryH-2.

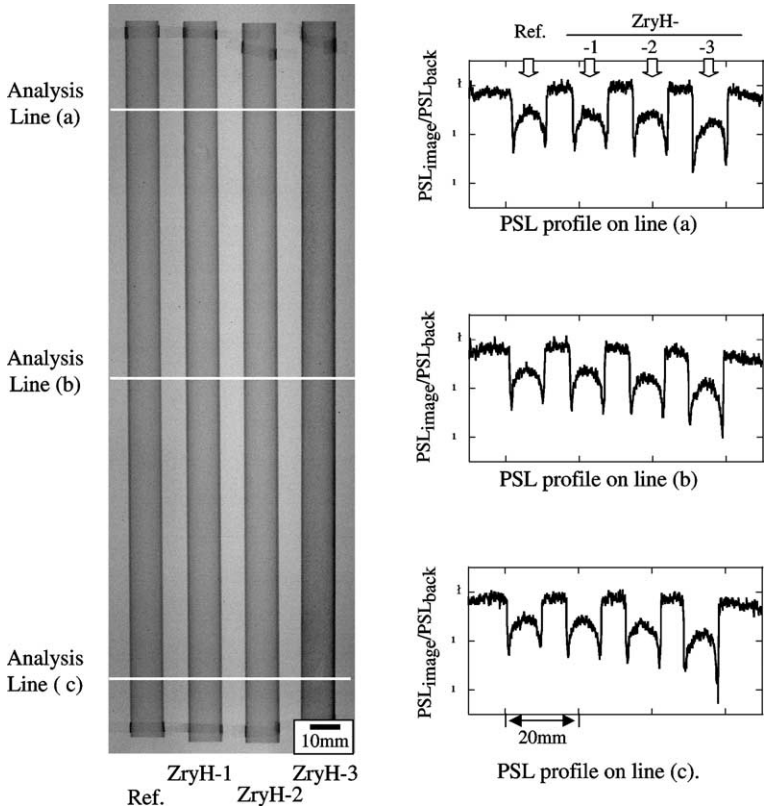

Fig. 4. The image at the left shows the rod image of hydrided tubes as compared with that of the reference one. Three figures at right show plotted curves of PSL line profiles on upper, middle, and bottom positions of the cladding tubes.

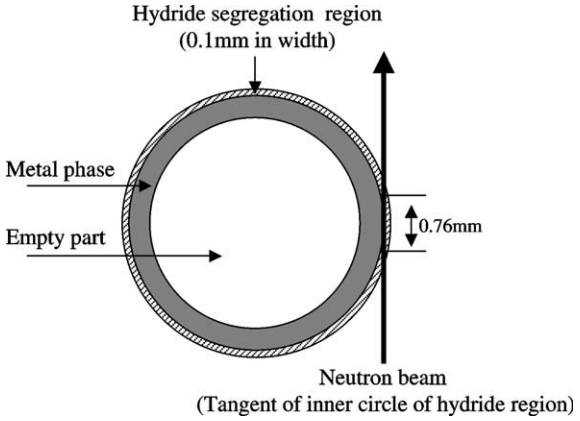

Fig. 5. Schematic drawing of path of primary neutron beam in a Zircaloy tube in the rod image examination.

On the other hand, the image of the ZryH-3 containing a large amount of hydrogen is visible to be dark when compared with the images of the other tubes. This results from scattering of the primary neutron beam by hydrogen. In the line profiles it however appears that the PSL_{image}/PSL_{back} slightly decreases with increasing hydrogen concentration. In the image of ZryH-3 the bottom part is definitely black when compared with the upper and middle parts. PSL_{image}/PSL_{back} of the bottom part (line (c)) is also lower in comparison with that of the upper (line (a)) and middle (line (b)) parts. The gradient of the hydrogen concentration in the hydrided tube caused the gradation and the change in the PSL_{image}/PSL_{back}.

Contributions of the introduced hydrogen are small in the rod images of ZryH-1 and ZryH-2 as shown in Fig. 4. Fig. 5 shows the schematic drawing of the geometric relationship between the tubes and primary neutron beam in the radiography examination of the rod image. The thickness of the Zircaloy-4 tubes and the width of the hydride region are 0.58 mm and around 0.1 mm, respectively. The longest length of the hydride region passed by the primary neutron beam is on the tangent of the inner hydride belt circle. The length is around 0.76 mm. According to Eqs. (3) and (4), the contribution of the hydrogen to PSL_{image}/PSL_{back} i.e. $(1-\exp(-\sigma_H N_H t))$ is $\sim$0.08 when the length $t = 0.76$ mm, σ_H: microscopic cross-section of hydrogen = 20 barn, and the concentration = 3.89×10^{21} n/cm^3 equivalent to 1000 wt ppm (1000 wt ppm$\fallingdotseq$9 at.% in the case of hydrogen in the zirconium metal phase, which gen-

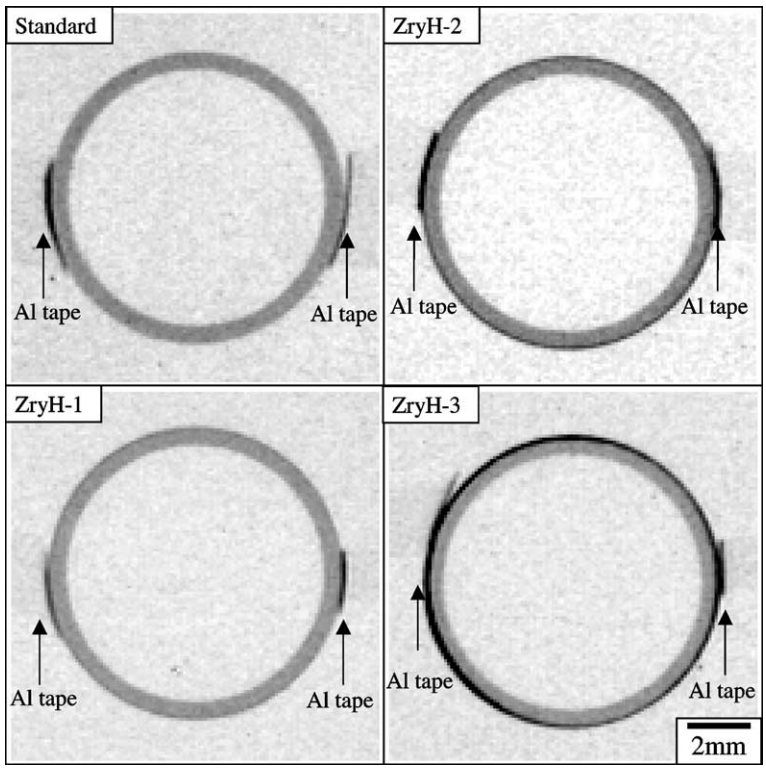

Fig. 6. Ring images of hydrided tubes.

erally corresponds to the concentration in the hydrided region in ZryH-2). The 0.08 is an appreciable value in changing the contrast in the image as shown in the line profiles in Fig. 4. The passed length of the primary neutron beam however shortens in the edge area in the side of the tubes. In addition, the spatial resolution of 0.1 mm × 0.1 mm in the IP image is insufficient to characterize the hydrided region around 0.1 mm in width. After a burn-up of 40 GW$d/t$ the concentration of the hydrogen in a Zircaloy tube is presumed to be around 300 wt ppm [9]. It appears that it is difficult to detect the hydrogen concentration by using the IP as evidenced from the present results. Improvements including S/N ratio and the spatial resolution in the IP system are needed to obtain the hydrogen behavior from the rod image.

Fig. 6 shows the ring images of the hydrided tubes examined by IP method. A black belt is recognized at the periphery in the ring images of the hydrided tubes. The black belt area corresponds to the hydrided region. The degree of darkness in the belt is enhanced with increasing the amount of the hydrogen concentration. There is a gradation in the black belts in the images of ZryH-2 and ZryH-3. The gradation indicates the gradient of hydrogen concentration. Line profiles of PSL_{image}/PSL_{back} in the ring images in Fig. 6 are shown in Fig. 7. The configuration of the curve of the reference tube is shown as a symmetric hollow. In the curve of the

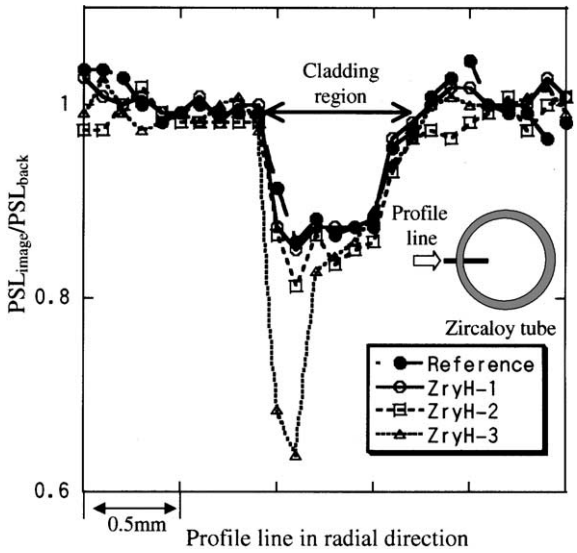

Fig. 7. Distribution of PSL_{image}/PSL_{back} in the hydrided tubes in the radial direction in the ring images.

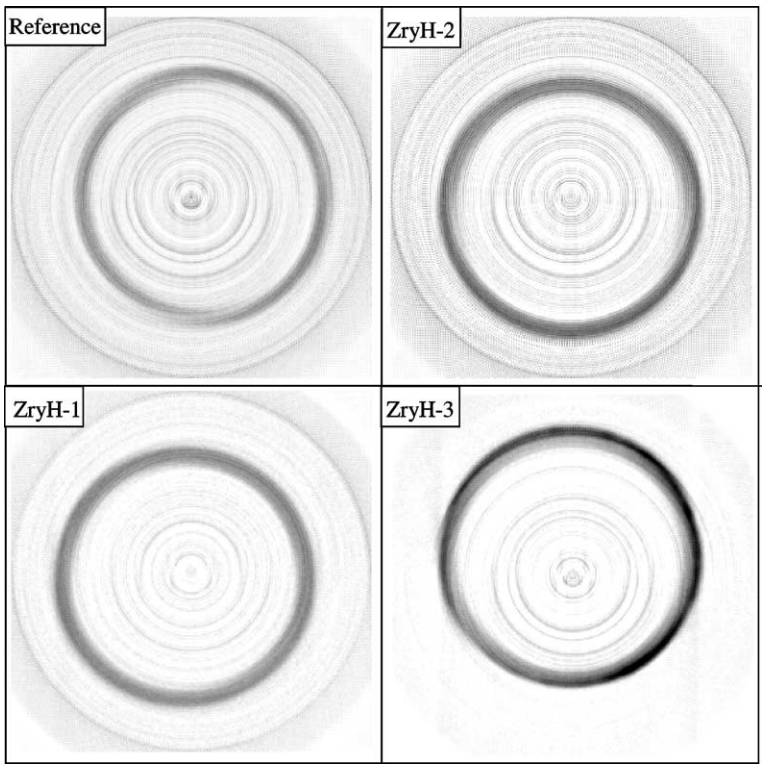

Fig. 8. CT images of hydrided and reference tubes.

hydrided tubes, the minimum of the PSL_{image}/PSL_{back} is positioned in the hydrogen segregation region. The minimum PSL_{image}/PSL_{back} decreases with increasing the hydrogen concentration. These are significant results in that the local distribution of the hydrogen concentration in the radial and circumferential directions is obtained. It appears that the neutron IP method may be a useful means as non-destructive hydrogen analysis prior to some mechanical testing such as ring tensile tests in which information about hydrogen concentration in the gauge parts is needed.

3.2. CT method

Fig. 8 shows the CT images of the hydrided tubes and the reference one. For improving the contrast of the CT images, the pictures in Fig. 8 are actually constructed by putting together 100 pictures. An obvious black belt caused by highly enriched hydrogen is confirmed at the hydrided region in the ZryH-3 image, and is obscured in the others. The black belt in ZryH-3 is even recognized in the CT image in a slice of 0.04 mm in thickness. By using CT method it shows that the 3D distribution of hydrogen concentration is nondestructively obtained with the spatial resolution of $0.04 \times 0.04 \times 0.04$ mm in an entire tube. Fig. 9 shows a line profile of CT numbers on the images of the cladding part in radial direction. The peaks of the profile curves of the hydrided tubes are positioned in the hydrided region, and the CT number of the peak increase with increasing the hydrogen concentration. The results show that the distribution of hydrogen concentration is confirmed numerically, even if the hydrided region is not recognized in the images. It is concluded that the neutron CT method is one of the effective tools to assess the hydrogen distribution.

3.3. Quantitative evaluation of hydrogen concentration

Fig. 10 shows the relationship between the PSL_{image}/PSL_{back} in the IP images of the hydrided tubes and its hydrogen concentrations. The repetitive tests were performed three times; i.e., test 1, test 2 and test 3. The PSL_{image}/PSL_{back} on the ordinate in Fig. 10 is introduced from average PSL_{image} on the overall ring images and average PSL_{back} on no sample images. Both PSLs are obtained from the same position in the image. All plotted curves indicate that the PSL_{image}/PSL_{back} decreases with increasing hydrogen concentration linearly. It is easy to estimate hydrogen concentration in Zircaloy tubes in the range from 300 to 1500 ppm by interpolating the curves. No large shift is shown among the plotted curves of test 1, test 2, and test 3 in Fig. 10, although there are slight differences in each test. The reproducibility in the tests is hence shown.

Fig. 11 shows the relationship between the CT number in the tube image and the hydrogen concentra-

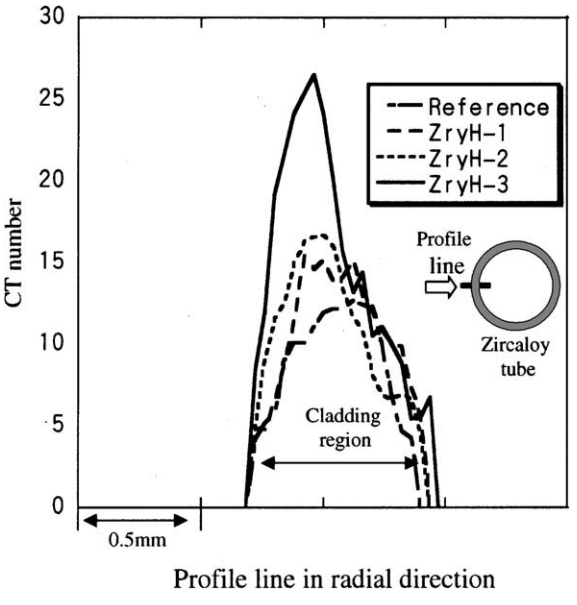

Fig. 9. Line profile of CT number in the hydrided tubes in the radial direction.

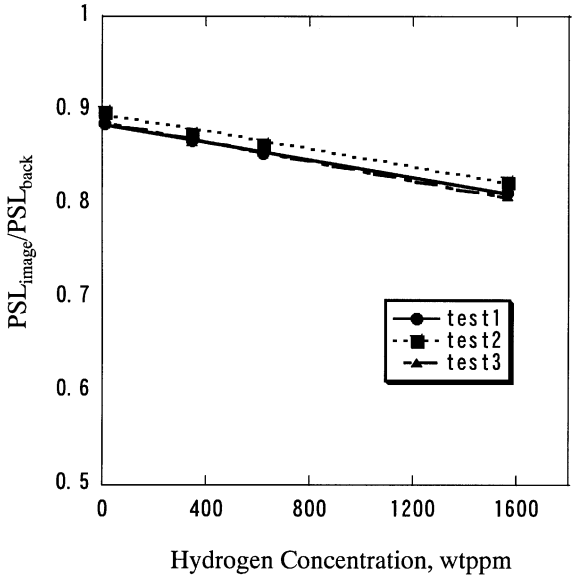

Fig. 10. Correlation between PSL_{image}/PSL_{back} in the ring image of hydrided tubes and the hydrogen concentration. The samples were cut from the inlet side of each tube.

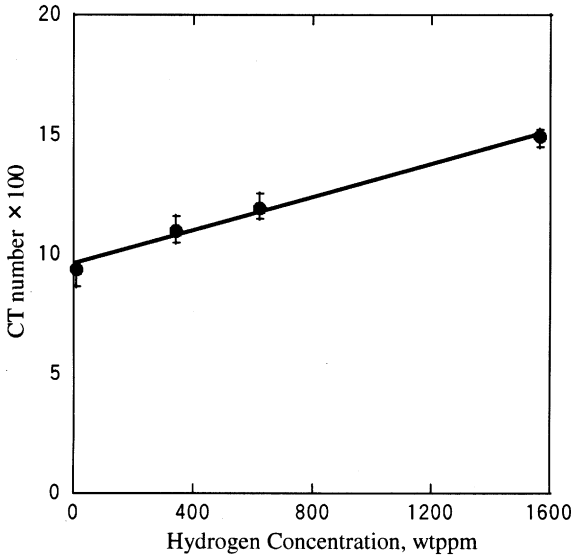

Fig. 11. Correlation between CT number on the CT images of hydrided tubes and the hydrogen concentration. The plotted marks are averaged CT numbers of a slice of CT image in 100 pieces. Error bars are introduced from maximum and minimum CT number of a slice of CT image in 100 pieces.

tion on the each image in Fig. 8. The plotted CT numbers on the ordinate in Fig. 11 are averaged all over the CT image of each tube. The hydrogen concentrations in Fig. 11 are averaged concentrations of the inlet and the outlet sides given in Table 2. This is justified because the CT images are obtained in the center of the tubes. The CT number linearly increases with increasing hydrogen concentration. Hydrogen concentration in the Zircaloy tube can be easily estimated on the plotted curve in the range of the tested hydrogen concentration. The mesh thickness of one CT image is around 0.04 mm as shown in Fig. 3. Hydrogen analysis using high temperature extraction methods usually needs a large sample of around 1 mm in thickness, being an irreversible and destructive process. We therefore consider that the neutron CT method is a nondestructive and effective tool for evaluating hydrogen concentration in a small area.

It is predicted that intense γ radiations from fission products (FPs) and from activated materials contribute to the images when these methods are used for PIE. Both IP itself and the CCD-camera are highly sensitive to γ-rays, and must detect them as backgrounds or noises. The present tests were performed on unirradiated and pre-hydrided cladding tubes without fuel pellets. Irradiated fuel pellets contain elements with large cross-sections, including U-235 and some FPs. Development of techniques and imaging processes for reducing the contribution of γ-rays and the nuclei with large cross-sections to the image are important subjects for PIE application.

4. Summary

The results are summarized in the following.

(1) Imaging plate: The gradient of the hydrogen concentration is confirmed in the rod image of the tubes ZryH-3 with high concentration of hydrogen, although not in the other tubes. An appreciable black belt caused by hydrogen is confirmed at the periphery in the ring images of all hydrided tubes under the present conditions. A linear relationship between the PSL_{image}/PSL_{back} and hydrogen concentration in the Zircaloy tubes is obtained. Those results show that IP method is one of the effective tools for estimating hydrogen concentration in Zircaloy tubes.

(2) CT method: The contribution of hydrogen is shown in the CT image of ZryH-3 tube that contained large amount of the hydrogen. Line profiles of CT number in the CT images of the hydrided tubes show that the peaks are positioned in the hydrogen segregation region. Similar to the results of IP, a linear relationship between the CT number and the hydrogen concentration is obtained. CT method will also provide an effective means of estimating hydrogen concentration in Zircaloy tubes.

Acknowledgements

The authors are deeply grateful to Dr Tsuneo Kodaira, Messrs Masami Shindo, Hidetoshi Amano, Yasuharu Nishino, and Dr Fumihisa Nagase for valuable advice and useful discussions. They are indebted to Hitoshi Andou and the staff members of the Department of Research Reactor for technical support in the examinations. They are grateful to Messrs Ishio Takahashi, Yuichi Hatakeyama, and the staff members of Department of Hot Laboratories for technical support in sample preparation and hydrogen analysis.

References

[1] H. Sakaguchi, A. Kohzai, K. Hatakeyama, S. Fujine, K. Yoneda, K. Kanda, T. Esaka,, Int. J. Hydrogen Energy 25 (2000) 1205.
[2] M. Zanarini, P. Chirco, M. Rossi, G. Bladazzi, G. Guidi, E. Querzola, M.G. Scannavini, F. Casali, IEEE Trans. Nucl. Sci. 42 (4) (1995) 580.
[3] J. Rant, I. Kodeli, G. Pregl, F. Zitnk, Proceeding of the 3rd WCNR (1989) 289.

[4] H.H. Klepfer, H.D. Kosanke, E.L. Esch, ASTM STP 458, Applications Related Phenomena in Zirconium and its Alloys (1969) p. 372.
[5] M. Matsubayashi, A. Tsuruno, T. Kodaira, H. Kobayashi, Nucl. Instr. and Meth. 377 (1996) 107.
[6] N. Niimura, Y. Karasawa, I. Tanaka, J. Miyahara, K. Takahashi, H. Saito, S. Koizumi, M. Hidaka, Nucl. Instrum. and Meth. 349 (1994) 521.
[7] F. Nagase, T. Otomo, H. Uetsuka, Japan Atomic Energy Research Institute Reports, JAERI-Research 2000-46 Dec.2000 (in Japanese).
[8] J.P. Barton, (Ed.), Neutron Radiography, Proceedings of the first WCNR, 1983, p. 899.
[9] D. Deydier, Corrosion Behavior of Zircaloy 4 Fuel Rod Cladding in EDF Power Plants, in: IAEA Technical Committee Meeting, Rez near Prague, Czech Republic, October, 1993.